ORGANIC LETTERS

2009
Vol. 11, No. 17
3850−3853

Facile Synthesis of Spirocyclic Aromatic Hydrocarbon Derivatives Based on *o*-Halobiaryl Route and Domino Reaction for Deep-Blue Organic Semiconductors

Feng Liu,[†] Ling-Hai Xie,[†] Chao Tang,[†] Jing Liang,[†] Qing-Quan Chen,[†] Bo Peng,[†] Wei Wei,*[,†] Yong Cao,[‡] and Wei Huang*[,†]

Jiangsu Key Lab for Organic Electronics & Information Displays and Institute of Advanced Materials (IAM), Nanjing University of Posts & Telecommunications (NUPT), 9 Wenyuan Road, Nanjing 210046, China, and Institute of Polymer Optoelectronic Materials and Devices, South China University of Technology, Guangzhou 510640, China

wei-huang@njupt.edu.cn; iamww@fudan.edu.cn

Received June 24, 2009

ABSTRACT

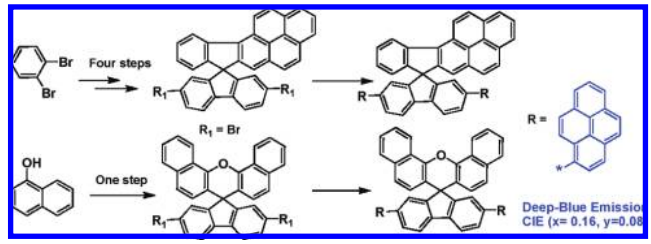

Conventional *o*-halobiaryl and one-pot tandem protocols have been developed to synthesize naphthalene- and pyrene-containing spirofluorenes. Two pyrene substituents were installed using a Suzuki cross-coupling reaction to produce a series of spirofluorene-functionalized polycyclic aromatic hydrocarbon derivatives, DPSBFF, DPSIPF, DPSDBXF, and DPSFX. A preliminary spin-coated device based on DPSFX:PVK blends exhibits a low turn-on voltage of 4.3 V and deep-blue emission with a current efficiency of 1.1 cd/A.

Polycyclic aromatic hydrocarbons (PAHs) are important planar organic semiconductors for high-performance OFETs.[1,2] However, they are not favored in OLEDs due to the large red-shifted emission as well as concentration-quenching effect from solution to solid state. Recently, pyrene-functionalized materials were proven to be promising blue emitters because of their high photoluminescence efficiency, high carrier mobility, and improved hole-injecting ability.[3]

On the other hand, bulky spirofluorene building blocks, especially spirobifluorene (SBF), are widely used in opto-electronic materials due to their unique steric hindrance effect.[4] The introduction of spirofluorene frameworks into organic semiconductors could increase the thermal and morphological stability as well as carrier mobility.[5] Although novel spirofluorenes are continuously reported, there are few reports on spiro-functionalized polycyclic aromatic hydro-carbon (SPAH) derivatives. Incorporation of PAHs into cruciform spirobifluorenes is an effective method to control the $\pi-\pi$ stacking interactions, which significantly impacts the emission behaviors of devices.

[†] Nanjing University of Posts & Telecommunications.
[‡] South China University of Technology.

(1) Wu, J. S.; Pisula, W.; Mullen, K. *Chem. Rev.* **2007**, *107*, 718–747.
(2) Zaumseil, J.; Sirringhaus, H. *Chem. Rev.* **2007**, *107*, 1296–1323.

10.1021/ol900978x CCC: $40.75 © 2009 American Chemical Society
Published on Web 08/05/2009

So far, there have been several synthetic protocols to prepare spirofluorenes in the literature. One of the most popular protocols is the *o*-halobiaryl route, in which an *o*-halobiaryl anion first attacks fluorenone to form a corresponding tertiary alcohol and is then followed by Friedel–Crafts cyclization.[6] With this method, various specified spirofluorenes could be obtained by designing symmetric and asymmetric *o*-halobiaryls. Yet this method requires laborious multistep reactions.[7] Recently, a one-pot tandem preparation strategy for spirofluorenes was reported.[8,9] Spiro[fluorene-9,9′-xanthene] (SFX) was occasionally obtained in the preparation of 4,4′-(9-fluorenylidene)diphenol.[8] To the best of our knowledge, spiro[dibenzo[*c*,*h*]xanthene-7,9-fluorene] (SDBXF) is still unexplored. In this communication, we prepared a seire of spirocycle aromatic hydrocarbons (SCAHs), naphthalene- and pyrene-containing spirofluorenes, via conventional *o*-halobiaryls and one-pot tandem protocols. Their pyrene-functionalized derivatives are excellent blue light-emitting materials in solution-processable devices.

The asymmetric naphthalene- and pyrene-containing spirofluorene building blocks were synthesized using the *o*-bromobiaryl route as shown in Scheme 1. *o*-Bromobiaryls

Scheme 1. Synthesis Routes of DBrSBFF and DBrSPPF via the *o*-Bromodiaryl Intermadiates

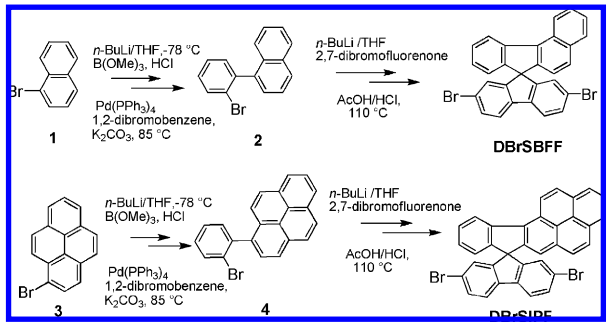

2 and **4** were synthesized via the Suzuki coupling reaction. This was followed by addition of 2,7-dibromofluorenone under *n*-BuLi conditions affording the corresponding tertiary alcohols. The crude products underwent dehydration cyclization to obtain the key SCAH building blocks 2′,7′-dibromospiro[benzo[*c*]fluorene-7,9′-fluorene] (DBrSBFF) and 2,7-dibromospiro[fluorene-9,7′-indeno[1,2-*a*]pyrene] (DBrSIPF).

According to our previous one-pot tandem protocol,[8] 2,7-dibromofluorenone and naphthalen-1-ol were stirred together under the conditions of methylsulfonic acid at 150 °C, and then 2′,7′-dibromospiro[dibenzo[*c*,*h*]xanthene-7,9-fluorene] (DBrSDBXF) was obtained in nearly stoichiometric yields, as shown in Scheme 2.

Scheme 2. One-Pot Procedures for DBrSDBXF

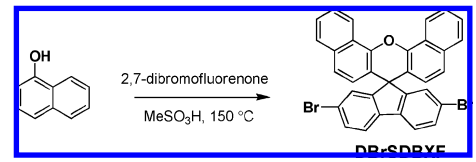

This key intermediate was reacted with 4,4,5,5-tetramethyl-2-(pyren-1-yl)-1,3,2-dioxaborolane using the Suzuki coupling reaction to afford the 2,7-dipyrene-functionalized organic semiconductors (Scheme 3). ^{1}H NMR and MALDI-TOF-

Scheme 3. Synthesis of Pyrene-Functionalized Final Products

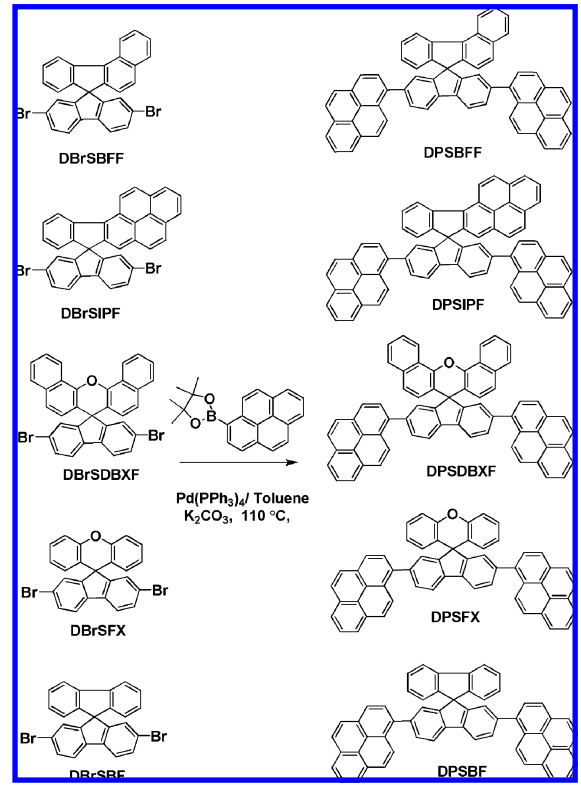

MS were used to characterize their structures (Supporting Information). Among these SPAHs, DPSBF was used for comparison.[10] DPSBFF and DPSIPF possess asymmetric SCAHs. DPSFX and DPSDBXF contain an oxygen atom in the SCAHs.

(3) (a) Liu, F.; Tang, C.; Chen, Q. Q.; Shi, F. F.; Wu, H. B.; Xie, L. H.; Peng, B.; Wei, W.; Cao, Y.; Huang, W. *J. Phys. Chem. C* **2009**, *113*, 4641–4647. (b) Liu, F.; Tang, C.; Chen, Q. Q.; Li, S. Z.; Wu, H. B.; Xie, L. H.; Peng, B.; Wei, W.; Cao, Y.; Huang, W. *Org. Electron.* **2009**, *10*, 256–265. (c) Liu, F.; Lai, W. Y.; Tang, C.; Wu, H. B.; Chen, Q. Q.; Peng, B.; Wei, W.; Huang, W.; Cao, Y. *Macromol. Rapid Commun.* **2008**, *29*, 659–664. (d) Tang, C.; Liu, F.; Xia, Y. J.; Xie, L. H.; Wei, A.; Li, S. B.; Fan, Q. L.; Huang, W. *J. Mater. Chem.* **2006**, *16*, 4074–4080. (e) Tang, C.; Liu, F.; Xia, Y. J.; Lin, J.; Xie, L. H.; Zhong, G. Y.; Fan, Q. L.; Huang, W. *Org. Electron.* **2006**, *7*, 155–162.

(4) (a) Saragi, T. P. I.; Spehr, T.; Siebert, A.; Fuhrmann-Lieker, T.; Salbeck, J. *Chem. Rev.* **2007**, *107*, 1011–1065. (b) Chiang, C. L.; Shu, C. F.; Chen, C. T. *Org. Lett.* **2005**, *7*, 3717–3720.

(5) Wu, C. C.; Liu, W. G.; Hung, W. Y.; Liu, T. L.; Lin, Y. T.; Lin, H. W.; Wong, K. T.; Chien, Y. Y.; Chen, R. T.; Hung, T. H.; Chao, T. C.; Chen, Y. M. *Appl. Phys. Lett.* **2005**, *87*, 052103.

The absorption spectra of DPSBF and DPSFX exhibit quite similar profiles (Figure 1) since the SPAHs possess

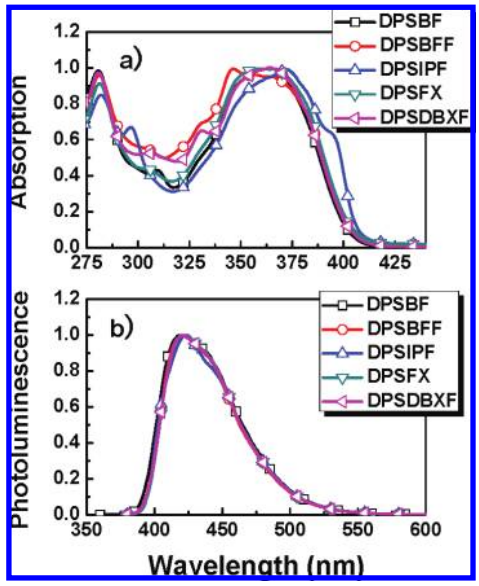

Figure 1. (a) Absorption spectra of SPAHs in dilute $CHCl_3$ solution (10^{-6} M). (b) Photoluminescence spectra of SPAHs in dilute $CHCl_3$ solution (10^{-6} M) excited using the maximum absorption wavelength.

the same main backbone of pyrene−fluorene−pyrene. The oxygen atom in the SCAH has a very weak effect on main chain conjugation and electronic structure of the materials. The absorption of DPSDBXF is close to DPSBFF, but the latter possesses an obvious new peak at 340 nm which can be attributed to a covalently conjugated connection between the naphthalene and benzene groups in the SCAH. DPSIPF is different from the other SPAHs, with a max absorption peak at 371 nm and an absorption shoulder at about 400 nm, suggesting that by enlarging the conjugation of the SCAH, the electronic structure of the conjugated backbone could be affected. The photoluminescence spectra of these molecules are nearly identical with the peak at 422 nm. DPSIPF shows a little difference, because of its large conjugated SCAH. The electrochemical behaviors of these materials were investigated by cyclic voltammetry. The onset oxidation peaks (E_{ox}) for DPSBF, DPSFX, DPSDBXF, DPSBFF, and DPSIPF were 0.84, 0.88, 0.82, 0.81, and 0.79 eV, respectively. Their HOMO energy levels were estimated to be −5.55, −5.59, −5.53, −5.52, and −5.50 eV.[11] For DPSBF, DPSBFF, and DPSIPF, while increasing the conjugation of the SCAH, the HOMO energy level slightly increased. From their UV−vis absorption edges, their band gap (ΔE_{abs}) was determined to be 2.98 eV. Thus, the LUMO was calculated. The corresponding data are summarized in Table 1.

Table 1. Physical Properties of Target Molecules

molecule	$\lambda_{abs,max}$ (nm)	$\lambda_{PL,max}$ (nm)	ΔE_{abs} (eV)	abs edge (nm)	HOMO (eV)	LUMO[a] (eV)
DPSBF	364	421	2.98	416	−5.55	−2.57
DPSBFF	364	422	2.98	416	−5.52	−2.54
DPSIPF	371	424	2.98	416	−5.50	−2.52
DPSFX	364	422	2.98	416	−5.59	−2.61
DPSDBXF	365	422	2.98	416	−5.53	−2.55

[a] LUMO = HOMO − ΔE_{abs} (band gap).

Quantum chemistry was employed to study the electronic structure of these materials. The molecules were optimized using the DFT/B3LYP method at a 6-31G level; the Zindo/S method was used to estimate the transition energies (ΔE_t) and the oscillator strength (I). The data are summarized in Table 2.

Table 2. Calculated HOMO, LUMO, and the Energy Gap (ΔE /eV) by B3LYP/6-31G Method

molecule	HOMO	LUMO	ΔE_{calc}	ΔE_t	intensity	H^{hole} (meV)	$H^{electron}$ (meV)
DPSBF	−5.136	−1.667	3.469	3.182	1.904	154	220
DPSBFF	−5.133	−1.667	3.466	3.173	1.896	156	218
DPSIPF	−5.132	−1.724	3.408	3.116	0.702	101	126
DPSFX	−5.167	−1.700	3.467	3.179	1.915	152	223
DPSDBXF	−5.161	−1.697	3.464	3.179	1.909	157	226

DPSFX and DPSDBXF show lower HOMO/LUMO than DPSBF due to the introduction of an oxygen atom. DPSIPF shows lower LUMO compared to DPSBF, indicating that the SCAH with more extensive conjugation could increase the electron affinity of the materials. In the Zindo/S calculations, DPSBF, DPSFX, DPSDBXF, and DPSBFF show similar transition energies and oscillator strength. DPSIPF shows lower transition energy and smaller oscillation intensity. The second lowest transition of DPSIPF shows an intensity of 1.980 (Supporting Information). Combined with the absorption study, we could ascribe the 400 nm absorption

(6) (a) Yu, W. L.; Pei, J.; Huang, W.; Heeger, A. J. *Adv. Mater.* **2000**, *12*, 828–831. (b) Xie, L. H.; Fu, T.; Hou, X. Y.; Tang, C.; Hua, Y. R.; Wang, R. J.; Fan, Q. L.; Peng, B.; Wei, W.; Huang, W. *Tetrahedron Lett.* **2006**, *47*, 6421–6424. (c) Xie, L. H.; Hou, X. Y.; Hua, Y. R.; Huang, Y. Q.; Zhao, B. M.; Liu, F.; Peng, B.; Wei, W.; Huang, W. *Org. Lett.* **2007**, *9*, 1619–1622. (d) Londenberg, J.; Saragi, T. R. L.; Suske, I.; Salbeck, J. *Adv. Mater.* **2007**, *19*, 4049–4053.

(7) (a) Luo, J.; Zhou, Y.; Niu, Z. Q.; Zhou, Q. F.; Ma, Y. G.; Pei, J. *J. Am. Chem. Soc.* **2007**, *129*, 11314–11315. (b) Chen, C. T.; Wei, Y.; Lin, J. S.; Moturu, M.; Chao, W. S.; Tao, Y. T.; Chien, C. H. *J. Am. Chem. Soc.* **2006**, *128*, 10992–10993.

(8) Xie, L. H.; Liu, F.; Tang, C.; Hou, X. Y.; Hua, Y. R.; Fan, Q. L.; Huang, W. *Org. Lett.* **2006**, *8*, 2787–2790.

(9) (a) Tseng, Y. H.; Shih, P. I.; Chien, C. H.; Dixit, A. K.; Shu, C. F.; Liu, Y. H.; Lee, G. H. *Macromolecules* **2005**, *38*, 10055–10060. (b) McFarlane, S. L.; Coumont, L. S.; Piercey, D. G.; McDonald, R.; Veinot, J. G. C. *Macromolecules* **2008**, *41*, 7780–7782.

(10) Tao, S. L.; Peng, Z. K.; Zhang, X. H.; Wang, P. F.; Lee, C. S.; Lee, S. T. *Adv. Funct. Mater.* **2005**, *15*, 1716–1721.

(11) Sun, Q. J.; Wang, H. Q.; Yang, C. H.; Li, Y. F. *J. Mater. Chem.* **2003**, *13*, 800–806.

shoulder to the lowest transition (S_0-S_1) and the maximum absorption at 371 nm to the second lowest transition (S_0-S_2). Thus, when the conjugation of the SCAH reached a certain extent, the frontier orbital and transition state of the material would be affected. Actually, the LUMO of DPSIPF is dominated by the SCAH, which is different from other materials (Supporting Information).

The Marcus theory was used to evaluate charge migration of these materials,[12] and the data are summarized in Table 2 (Supporting Information). Reorganization energies for hole and electron are quite similar for DPSBF, DPSFX, DPSDBXF, and DPSBFF. However, DPSIPF shows a much smaller value for both hole and electron. Although they have the same backbone, the conjugated SCAH for DPSIPF has a much stronger effect in affecting the electronic structure, leading to a decreased reorganization energy, and providing a better carrier transporting properties.

A spin-coated OLED device was fabricated by using DPSFX (5 wt %): PVK blends as the active layer. PBD (30 wt % compared to PVK) was added to increase electron mobility.[13] The device shows a deep-blue emission with CIE 1931 coordinates of ($x = 0.16$, $y = 0.08$). The electroluminescence is very close to that of DPSFX in solution. The turn-on voltage is 4.3 V and the maximum brightness is over 2000 cd/m^2. The peak current efficiency reaches 1.1 cd/A. Basic device performance shows that DPSFX is a promising light emitting material. Its potential could be fully explored by optimizing the device structure or using a vacuum deposition device fabrication method (Figure 2).

In conclusion, we have explored two different protocols to synthesize naphthalene- and pyrene-containing spirocycle aromatic hydrocarbons for novel nonplanar organic semiconductors. They show deep-blue emission and interesting device performance. Their electronic structure was studied by quantum chemistry and the carrier migration properties were analyzed by the Marcus theory. These priliminery results show that π-conjugated spirofluorene-functionalized PAHs are a promising family of organic semiconductors.

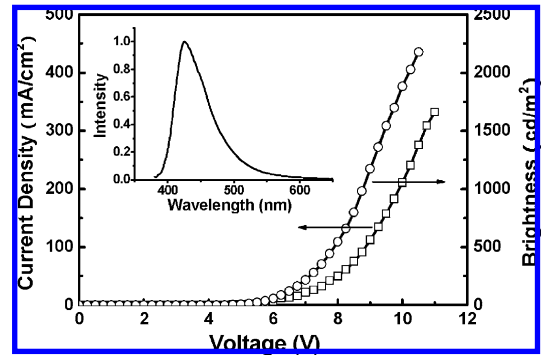

Figure 2. Performance of device with the configuration: [ITO/PEDOT:PSS (40 nm)/emitter (80 nm)/CsF (2 nm)/Al (90 nm)].

Acknowledgment. For financial support for this work, we thank the "973" project (2009CB930600), NNSFC (Grant Nos. 20704023, 60876010, 60706017, and 20774043), the Key Project of Chinese Ministry of Education (Nos. 208050 and 707032), and the NSF of the Education Committee of Jiangsu Province (Grant Nos. 07KJB150082, BK2008053, SJ209003, and TJ207035).

Supporting Information Available: Detailed synthetic procedures, NMR and MALDI-TOF-MS spectra, and molecular simulation. This material is available free of charge via the Internet at http://pubs.acs.org.

OL900978X

(12) Tant, J.; Geerts, Y. H.; Lehmann, M.; De Cupere, V.; Zucchi, G.; Laursen, B. W.; Bjornholm, T.; Lemaur, V.; Marcq, V.; Burquel, A.; Hennebicq, E.; Gardebien, F.; Viville, P.; Beljonne, D.; Lazzaroni, R.; Cornil, J. *J. Phys. Chem. B* **2005**, *109*, 20315–20323.

(13) Jiang, C. Y.; Yang, W.; Peng, J. B.; Xiao, S.; Cao, Y. *Adv. Mater.* **2004**, *16*, 537–541.

Supporting Information-*Organic Letters*

Facile Synthesis of Spirocyclic Aromatic Hydrocarbon Derivatives based on o-Halobiaryl Route and Domino Reaction for Deep-blue Organic Semiconductors

Feng Liu,[†] Ling-Hai Xie,[†] Chao Tang,[†] Jing Liang,[†] Qing-Quan Chen,[‡] Bo Peng,[†] Wei Wei, *,[†] Yong Cao,[‡] and Wei Huang *,[†]

Jiangsu Key Lab for Organic Electronics & Information Displays and Institute of Advanced Materials (IAM), Nanjing University of Posts & Telecommunications (NUPT), 9 Wenyuan Road, Nanjing 210046, China, and Institute of Polymer Optoelectronic Materials and Devices, South China University of Technology, Guangzhou 510640, China

* To whom all correspondence should be addressed. Phone: +86 25 8586 6008. Fax: +86 25 8586 6999. E-mail address: wei-huang@njupt.edu.cn/ iamww@fudan.edu.cn.

Experimental Section

Chemicals: *n*-BuLi, 2-bromopyrene, tetrakistriphenylphosphine palladium(0) were obtained from Aldrich Chemical Co. and were used without further purification. THF and diethyl ether were dried over sodium benzophenone ketyl anion radical and distilled under a dry nitrogen atmosphere immediately prior to use. 2,7-dibromo-9,9'-spirobi[fluorene] (DBrSBF), 2,7-dibromospiro [fluorene-9,9'-xanthene] (DBrSFX), 2-bromopyrene, 4,4,5,5-tetramethyl-2-(pyren-1-yl)-1,3,2-dioxaborolane, and 2,7-di(pyrenyl)spirobifluorene (DPSBF) were prepared as previously reported.[1]

Characterization: ^{1}H- and ^{13}C-NMR in $CDCl_3$ were recorded at 400 MHz using a Varian Mercury 400 plus spectrometer. Mass spectra was recorded with a Shimadzu GCMS-QP2010 plus spectrometer or a Shimadzu AXIMA-CFR plus spectrometer. Elemental analyses were carried out in an elementar Analysensysteme GmbH - vario EL III Element Analyzer. Absorption spectra (1 μM in $CHCl_3$) were measured with a Shimadzu UV-3150 spectrometer at 25°C, and emission spectra (1 μM in $CHCl_3$) were recorded with a Shimadzu RF-530XPC luminescence spectrometer upon excitation at the absorption maxima in the argon-degassed CH_2Cl_2 solvent. Differential scanning calorimetry (DSC) analyses were performed in a Shimadzu DSC-60A instrument, in which the sample was heated (10 °C/min) to 360 °C and then quenched with liquid nitrogen followed by heating (10°C/min) the quenched sample during spectra collection. Thermogravimetric analyses (TGA) were conducted by a Shimadzu DTG-60H under a heating rate of 10°C/min and a nitrogen flow rate of 20 cm^3/min. Cyclic

1. (a) Xie L. H.; Fu T.; Hou X. Y.; Tang C.; Hua Y. R.; Wang R. J.; Si S. M.;Fan Q. L.; Lian-Hui Wang, Wei Wei, Bo Peng, and Huang W. *Tetrahedron Letters* **2006**, *47* (36), 6421. (b) Thompson, A. L. H.; Attar, A. A.; Diasb, F. B.; Monkman, A. P. *J. Mater. Chem.* **2006**, *16*, 1046-1052. (c) Tsuboyama, A.; Iwawaki, H.; Furugori, M.; Mukaide, T.; Kamatani, J.; Igawa, S.; Moriyama, T.; Miura, S.; Takiguchi, T.; Okada, S.; Hoshino, M.; Ueno, K. *J. Am. Chem. Soc.* **2003**, *125*, 12971-12979.

voltammetric (CV) studies were made using an Eco Chemie BV. Electrochemical instruments. A platinum-sheet working electrode, a platinum-wire counter electrode, and a silver/silver nitride ($Ag/AgNO_3$) reference electrode were used to form a three-electrode configuration. All electrochemical experiments were carried out with a scan rate of 0.1 V/s under the nitrogen atmosphere at room temperature in the CH_2Cl_2 solvent with 0.1 M tetrabutylammonium hexafluorophosphate (n-Bu_4NPF_6) as the supporting electrolyte.

Quantum chemistry calculation: The quantum chemical calculations were performed using Gaussian 03, B.04 program. The ground state geometries were optimized by DFT/B3LYP method at 6-31G level. The frontier orbital information is obtained. Zindo/S method was used to estimate the transition energies ($\mathbf{\Delta E_t}$) and oscillator strength (**I**), in the calculation, the lowest 12 transition states and their oscillator strength were considered. Charge migration in organic solid is regarded as the hopping process. The rate of the charge hopping rate k_{ET} can be estimated by Marcus formalism:

$$k_{ET} = \frac{4\pi^2}{h} t^2 \frac{1}{\sqrt{4\pi\lambda RT}} e^{-\lambda/4RT}$$

where λ is internal reorganization energy which corresponding to the sum of geometry relaxation energies upon going from the neutral-state geometry to the charged-state geometry and vice versa. t represents the strength of intermolecular electronic coupling (transfer integrals) between adjacent molecules, dictated largely by orbital overlap. Reorganization energies of the molecules are evaluated by DFT/B3LYP method using 6-31G base set and the calculated values for hole transport and electron transport are summarized in manuscript Table 2. The transfer integrals are evaluated as half the splitting of the HOMO [LUMO] level for holes [electrons] in a dimmer formed by two molecules in their ground state geometry. The dimmer model was built by stacking the pyrene groups face to face, and d is the intermolecular distance (Figure S6). The results are shown in Figure S7. The electronic splittings decrease exponentially when the intermolecular distance is increased. Short distances are thus desirable to promote high hopping rates. And generally transfer integral for hole is larger than transfer integral for electron.

Fabrication and characterization of Device: LED was fabricated on pre-patterned indium-tin oxide (ITO) with sheet resistance 10-20 Ω/□. The substrate was ultrasonic cleaned with acetone, detergent, deionized water, and 2-propanol. Oxygen plasma treatment was made for 5 min as the final step just before film coating. Onto the ITO glass was spin-coated a layer of polyethylenedioxythiophene-polystyrene sulfonic acid (PEDOT: PSS) film with thickness of 40 nm from its aqueous dispersion. PEDOT: PSS film was dried at 80 °C for 12 h in the vacuum oven. The solution of the polymer was prepared under nitrogen atmosphere and spin-coated on to PEDOT: PSS

layer. Typical thickness of the emitting layer was 80 nm and heated at 60 °C for 30 min. Then a thin layer of 2 nm CsF as the electron injection cathode and the subsequent 120 nm thick aluminum protection layers were thermally deposited by vacuum evaporation through a mask at a base pressure below 4×10^{-4} Pa. The cathode area defines the active area of the device. The typical active area of the devices in this study is 0.17 cm^2. The EL layer spin coating process and the device performance tests were carried out within a glove box under nitrogen atmosphere. Current-voltage (I-V) characteristics were recorded with a Keithley 236 source meter. EL spectra were measured by a PR 705 photometer (Photo Research). The external quantum efficiencies were determined by a Si photodiode with calibration in an integrating sphere (IS080, Labsphere).

Preparation of 1-(2-bromophenyl)naphthalene (2): 1-bromonaphthalene (4.14 g, 20 mmol) was dissolved in distillated THF (50 mL) in capped bottle. The temperature was kept in -78 ^oC using dry ice/acetone bath. BuLi (12.5 mL，20 mmol) was added to the bottle and stirred for 1.5 h under -78 ^oC. Then trimethyl borate (4.2 g, 50 mmol) was added quickly, stirr under -78 ^oC for 1.5 h and then run overnight under room temperature. HCl (2M, 200 ml) was added and stirred for 5 h. The solution was extracted with dichloromethane, washed with water, dried with anhydrous $MgSO_4$. The solvent was removed by rotary evaporation, white solid was obtained. 1,2-dibromobenzene (4.67g, 20 mmol) was added to the crude product, $Pd(PPh_3)_4$ (40mg), K_2CO_3 (2M, 10 ml) and degassed toluene (40 ml) were added. Run the reaction under 85 ^oC for 24 h under N_2 without light exposure. The reaction solution was extracted with dichloromethane, washed with water, dried with anhydrous $MgSO_4$. The solvent was removed by rotary evaporation, and the residue was purified by column chromatography using CH_2Cl_2/petroleum ether (1 : 10) as eluent to obtain the white solid (3.34 g, 59%). ^{1}HNMR (400 MHz, $CDCl_3$) δ(ppm): 7.93 (d, 2H); 7.75 (d, 1H); 7.55 (t, 1H); 7.51-7.40 (m, 4H); 7.38 (d, 2H); 7.32 (t, 1H). MALDI-TOF-MS (m/z): Calcd. for $C_{16}H_{11}Br$ 283.2, found 283.4.

Preparation of 1-(2-bromophenyl)pyrene (4): 1-bromopyrene (2.81 g, 10 mmol) was dissolved in distillated THF (30 mL) in capped bottle. The temperature was kept in -78 ^oC using dry ice/acetone bath. BuLi (6.25 mL, 10 mmol) was added to the bottle and stirred for 1.5 h under -78 ^oC. Then trimethyl borate (2.1 g, 25 mmol) was added quickly, stirr under -78 ^oC for 1.5 h and then run overnight under room temperature. HCl (2M, 100 ml) was added and stirred for 5 h. The solution was extracted with dichloromethane, washed with water, dried with anhydrous $MgSO_4$. The solvent was removed by rotary evaporation, white solid was obtained. 1,2-dibromobenzene (2.33g, 10 mmol) was added to the crude product, $PdP(Ph_3)_4$ (40mg), K_2CO_3 (2M, 10 ml) and degassed toluene (40 ml) were added. Run the reaction under 85 ^oC for 24 h under N_2 without light exposure. The reaction solution was extracted with dichloromethane, washed with water, dried with anhydrous $MgSO_4$. The solvent was removed by

rotary evaporation, and the residue was purified by column chromatography using CH_2Cl_2/petroleum ether (1 : 8) as eluent to obtain the white solid (2.28 g, 64%). ^{1}H-NMR (400 MHz, $CDCl_3$): δ (ppm) 8.29 (d, 1H), 8.25 (m 2H), 8.16 (d, 2H), 8.08 (m, 2H), 8.00 (d, 1H), 7.87 (m, 2H), 7.54 (m, 2H), 7.40(m, 1H). MALDI-TOF-MS (m/z): Calcd. for $C_{22}H_{13}Br$ 357.2, found 357.1.

Preparation of 2',7'-dibromospiro[benzo[c]fluorene-7,9'-fluorene] (DBrSBFF): 1-(2-bromophenyl)naphthalene (2) (2.83g, 10 mmol) was dissolved in dry THF (25 mL) in capped bottle. The temperature was kept in -78 ^{o}C using dry ice/acetone bath. BuLi (6.25 mL，10 mmol) was added to the bottle and stirred for 1.5 h under -78 ^{o}C. Then, the reaction solution was taken out by syringe and was added to 2,7-dibromofluorenone (3.37g, 10 mmol) THF solution. The reaction mixture was extracted with dichloromethane, washed with water, dried with anhydrous $MgSO_4$. The solvent was removed by rotary evaporation, white solid was obtained. The crude product was dissolved in AcOH, several drops of concentrated HCl was added. Keep the reaction under 110 ^{o}C for 24 h. The reaction solution was extracted with dichloromethane, washed with water, dried with anhydrous $MgSO_4$. The solvent was removed by rotary evaporation, and the residue was purified by column chromatography using CH_2Cl_2/petroleum ether (1 : 6) as eluent to obtain the white solid (3.88 g, 74%). ^{1}H-NMR (500 MHz, $CDCl_3$): δ (ppm) 8.85 (d, 1H), 8.45 (d 1H), 7.93 (d, 1H), 7.73-7.65 (m, 4H), 7.56 (t, 1H), 7.51 (d, 3H), 7.19 (t, 1H), 6.82-6.78(m, 4H). MALDI-TOF-MS (m/z): Calcd. for $C_{29}H_{16}Br_2$ 524.3, found 524.9.

Preparation of 2,7-dibromospiro[fluorene-9,7-indeno[1,2-a]pyrene] (DBrSIPF): 1-(2-bromophenyl)pyrene (4) (2.28g, 6 mmol) was dissolved in distillated THF (25 mL) in capped bottle. The temperature was kept in -78 ^{o}C using dry ice/acetone bath. *n*-BuLi (3.75 mL，6 mmol) was added to the bottle and stirred for 1.5 h under -78 ^{o}C. Then, the reaction solution was taken out by syringe and was added to 2,7-dibromofluorenone (2.02g, 6 mmol) THF solution. The reaction mixture was extracted with dichloromethane, washed with water, dried with anhydrous $MgSO_4$. The solvent was removed by rotary evaporation, white solid was obtained. The crude product was dissolved in AcOH, several drops of concentrated HCl was added. Keep the reaction under 110 ^{o}C for 24 h. The reaction solution was extracted with dichloromethane, washed with water, dried with anhydrous $MgSO_4$. The solvent was removed by rotary evaporation, and the residue was purified by column chromatography using CH_2Cl_2/petroleum ether (1 : 6) as eluent to obtain the white solid (2.48 g, 69%). ^{1}H-NMR (400 MHz, $CDCl_3$): δ (ppm) 9.12 (d, 1H), 8.66 (d 1H), 8.37 (d, 2H), 8.26 (d, 1H), 8.18 (t, 1H), 8.10-7.99 (m, 3H), 7.83-7.74 (m, 4H), 7.59-7.51(m, 4H), 7.25 (d, 1H), 6.88 (s, 2H). MALDI-TOF-MS (m/z): Calcd. for $C_{35}H_{20}Br_2$ 600.3, found 600.7.

Preparation of 2',7'-dibromospiro[dibenzo[c,h]xanthene-7,9-fluorene] (DBrSDBXF): A mixture of 2,7-dibromofluorenone (6.523 g, 19.3 mmol, 1 equiv), naphthalen-1-ol (11.116 g, 77.2 mmol, 4 equiv),

and methane sulfonic acid ($MeSO_3H$, 5.0 ml, 7.41 g, 77.2 mmol, 4 equiv) was heated at 150 °C under nitrogen for 24 h. the reaction mixture was then slowly add into water (50 ml) and extracted with dichloromethane. The combined extracts were dried over $MgSO_4$, evaporated, and recrystallized with ethyl acetate to afford white solid (9.34 g, 82%). ^{1}H-NMR (500 MHz, $CDCl_3$): δ (ppm) 8.77 (d, 2H), 7.78 (d, 2H), 7.74-7.69 (m, 4H), 7.59 (t, 2H), 7.53 (d, 2H), 7.31 (d, 2H), 7.27 (s, 2H), 6.38 (d, 2H). MALDI-TOF-MS (m/z): Calcd. for $C_{33}H_{18}Br_2O$ 590.3, found 590.7.

Preparation of 2,7-di(pyren-1-yl)spiro[fluorene-9,7-benzo[c]fluorene] (DPSBFF): In a 50 ml bottle, 4,4,5,5-tetramethyl-2-(pyren-1-yl)-1,3,2-dioxaborolane (1.0 g, 3.0 mmol), DBr-SNPF (0.786 g, 1.5 mmol), $Pd(PPh_3)_4$ (0.02 mmol), degassed toluene (50 mL) and K_2CO_3 (2 M, 10 ml) was added. The bottle was capped and protected with N_2. Light exposure was avoided. Run the reaction under 90 °C for 48 h. The reaction solution was extracted with dichloromethane. The solvent was removed by rotary evaporation, and the residue was purified by column chromatography using CH_2Cl_2/petroleum ether (1 : 4) as eluent to obtain the white solid (0.771 g, 67%). ^{1}H-NMR (500 MHz, $CDCl_3$): δ (ppm) 8.77 (d, 1H), 8.38 (d, 1H), 8.17-8.07 (m, 10H), 8.02-7.90 (m, 10H), 7.85 (d, 2H), 7.76 (d, 3H), 7.62 (t, 1H), 7.51 (t, 1H), 7.46 (t, 1H), 7.15 (t, 2H), 7.05 (s, 2H). MALDI-TOF-MS (m/z): Calcd. for $C_{61}H_{34}$ 766.9, found 767.4. Anal. Calcd. C, 95.53; H, 4.47. found C, 95.45; H, 4.51.

Preparation of 2,7-di(pyren-1-yl)spiro[fluorene-9,7-indeno[1,2-a]pyrene] (DPSIPF): In a 50 ml bottle, 4,4,5,5-tetramethyl-2-(pyren-1-yl)-1,3,2-dioxaborolane (1.0 g, 3.0 mmol), DBrSPPF (0.900 g, 1.5 mmol), $Pd(PPh_3)_4$ (0.02 mmol), degassed toluene (50 mL) and K_2CO_3 (2M, 10 ml) was added. The bottle was capped and protected with N_2. Light exposure was avoided. Run the reaction under 90 °C for 48 h. The reaction solution was extracted with dichloromethane. The solvent was removed by rotary evaporation, and the residue was purified by column chromatography using CH_2Cl_2/petroleum ether (1 : 4) as eluent to obtain the greenish white solid (0.971 g, 77%). ^{1}H-NMR (500 MHz, $CDCl_3$): δ (ppm) 8.66 (d, 1H), 8.31 (d, 1H), 8.22-8.11 (m, 8H), 8.06-7.92 (m, 16H), 7.85 (d, 2H), 7.76 (d, 2H), 7.65 (s, 1H), 7.50 (s, 1H), 7.40 (t, 1H), 7.20 (t, 1H), 7.08-7.03 (m, 2H). MALDI-TOF-MS (m/z): Calcd. for $C_{67}H_{36}$ 841.0, found 841.4. Anal. Calcd. C, 95.69; H, 4.31. found C, 95.49; H, 4.48.

Preparation of 2,7-di(pyren-1-yl)spiro[fluorene-9,9-xanthene] (DPSFX): In a 50 ml bottle, 4,4,5,5-tetramethyl-2-(pyren-1-yl)-1,3,2-dioxaborolane (1.0 g, 3.0 mmol), DBr-SFX (0.735 g, 1.5 mmol), $Pd(PPh_3)_4$ (0.02 mmol), degassed toluene (50 mL) and K_2CO_3 (2M, 10 ml) was added. The bottle was capped and protected with N_2. Light exposure was avoided. Run the reaction under 90 °C for 48 h. The reaction solution was extracted with dichloromethane. The solvent was removed by rotary evaporation, and the residue was purified by column chromatography using CH_2Cl_2/petroleum ether (1 : 4) as eluent to obtain the yellowish white solid (0.78 g, 72%). ^{1}HNMR (400 MHz, $CDCl_3$)δ(ppm): 8.19-8.13 (m, 6H); 8.09 – 8.07 (d, 8H); 8.02 - 7.91 (m, 6H); 7.75 - 7.73 (d, 2H); 7.54 (s, 2H); 7.24 -

7.17 (m, 4H); 6.95 (t, 2H); 6.81 (d, 2H). MALDI-TOF-MS (m/z): Calcd. for $C_{57}H_{32}O$ 732.9, found 733.2. Anal. Calcd. C, 93.42; H, 4.40; O, 2.18. found C, 93.25; H, 4.62.

Preparation of 2,7- di(pyren-1-yl)spiro[fluorene-9,7-dibenzo[c,h]xanthene] (DPSDBXF): In a 50 ml bottle, 4,4,5,5-tetramethyl-2-(pyren-1-yl)-1,3,2-dioxaborolane (1.0 g, 3.0 mmol), DBr-SNF (0.885 g, 1.5 mmol), $Pd(PPh_3)_4$ (0.02 mmol), degassed toluene (50 mL) and K_2CO_3 (2M, 10 ml) was added. The bottle was capped and protected with N_2. Light exposure was avoided. Run the reaction under 90 °C for 48 h. The reaction solution was extracted with dichloromethane. The solvent was removed by rotary evaporation, and the residue was purified by column chromatography using CH_2Cl_2/petroleum ether (1 : 4) as eluent to obtain the white solid (0.962 g, 77%). ^{1}HNMR (400 MHz, $CDCl_3$)δ(ppm): 8.70 (d, 2H); 8.15 (t, 4H); 8.07 (m, 6H); 8.01 (s, 4H); 7.95 (t, 2H); 7.88 - 7.76 (m, 8H); 7.63 (t, 2H); 7.53 (d, 4H); 7.46 (d, 2H); 6.82 (d, 2H). MALDI-TOF-MS (m/z): Calcd. for $C_{65}H_{36}O$ 833.0, found 833.4. Anal. Calcd. C, 93.72; H, 4.36; O, 1.92. found C, 93.65; H, 4.42.

Table S1. ZINDO/SCI calculated lowest transition energies (ΔE_t /eV) and oscillator strengths (I /a.u.)

Excited	DPSBF		DPSBFF		DPSIPF	
State	ΔE_t	*I*	ΔE_t	*I*	ΔE_t	*I*
1	3.1816	*1.9035*	3.1732	*1.8955*	3.1157	*0.7025*
2	3.2939	*0.0691*	3.2906	*0.0934*	3.1764	*1.9802*
3	3.3106	*0.0514*	3.3096	*0.0505*	3.2285	*0.1237*
4	3.3330	*0.0512*	3.3293	*0.0605*	3.2952	*0.0522*
5	3.7583	*0.3699*	3.5196	*0.3168*	3.3099	*0.0485*
6	4.0135	*0.2433*	3.7289	*0.0317*	3.3343	*0.0524*
7	4.0171	*0.0129*	3.7427	*0.3485*	3.7499	*0.3497*
8	4.0301	*0.0010*	4.0093	*0.0224*	3.9683	*0.2159*
9	4.0537	*0.0009*	4.0262	*0.0027*	4.0119	*0.0195*
10	4.1019	*0.0201*	4.0497	*0.0022*	4.0276	*0.0016*
11	4.2242	*0.0034*	4.0934	*0.0261*	4.0436	*0.0023*
12	4.3316	*0.0126*	4.1636	*0.0002*	4.0512	*0.0027*

Table S2. ZINDO/SCI calculated lowest transition energies (ΔE_t /eV) and oscillator strengths (I /a.u.)

Excited	DPSFX		DPSDBXF	
State	ΔE_t	*I*	ΔE_t	*I*
1	3.1791	*1.9152*	3.1787	*1.9093*
2	3.2943	*0.0699*	3.2921	*0.1006*
3	3.3108	*0.0479*	3.3105	*0.0480*
4	3.3322	*0.0506*	3.3288	*0.0641*
5	3.7465	*0.3532*	3.7368	*0.0906*
6	4.0034	*0.0172*	3.7469	*0.0004*
7	4.0290	*0.0011*	3.7549	*0.3686*
8	4.0490	*0.0001*	3.7812	*0.0995*
9	4.0953	*0.0156*	3.9864	*0.0758*
10	4.3121	*0.0315*	4.0301	*0.0008*
11	4.3227	*0.0159*	4.0439	*0.0166*
12	4.3469	*0.1150*	4.0579	*0.0469*

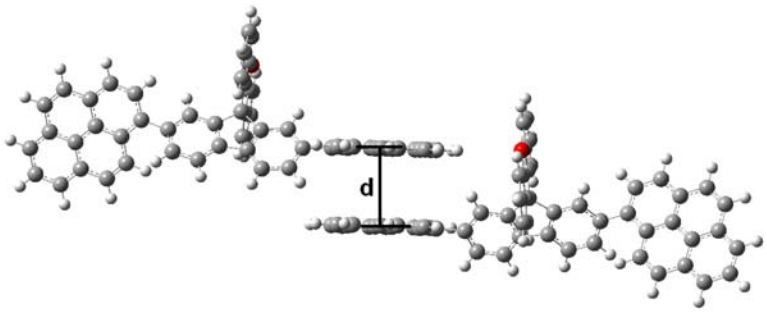

Figure S-1. Pyrene stacked dimmer model of DPSFX

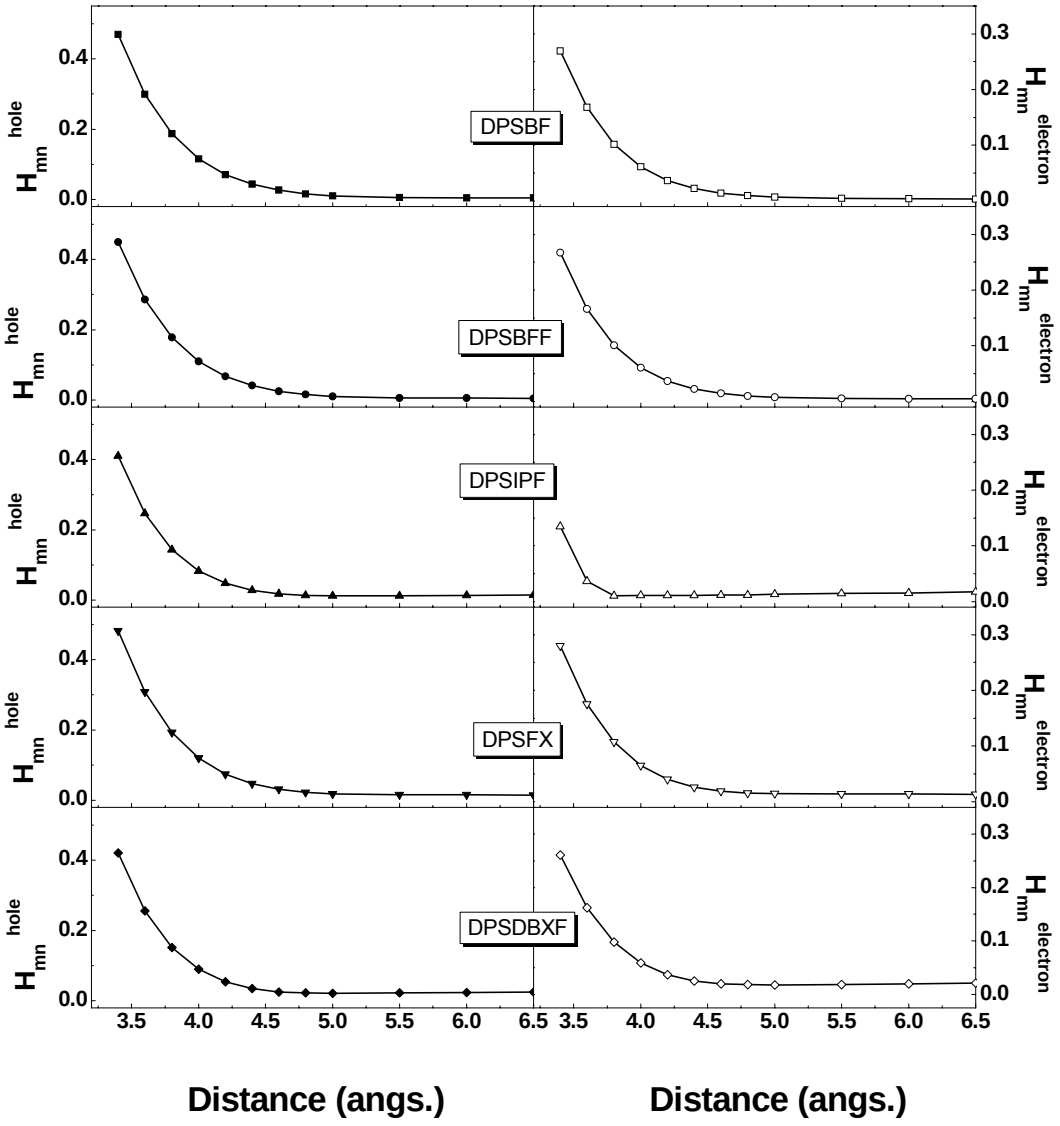

Figure S-2. Transfer integrals of the molecules

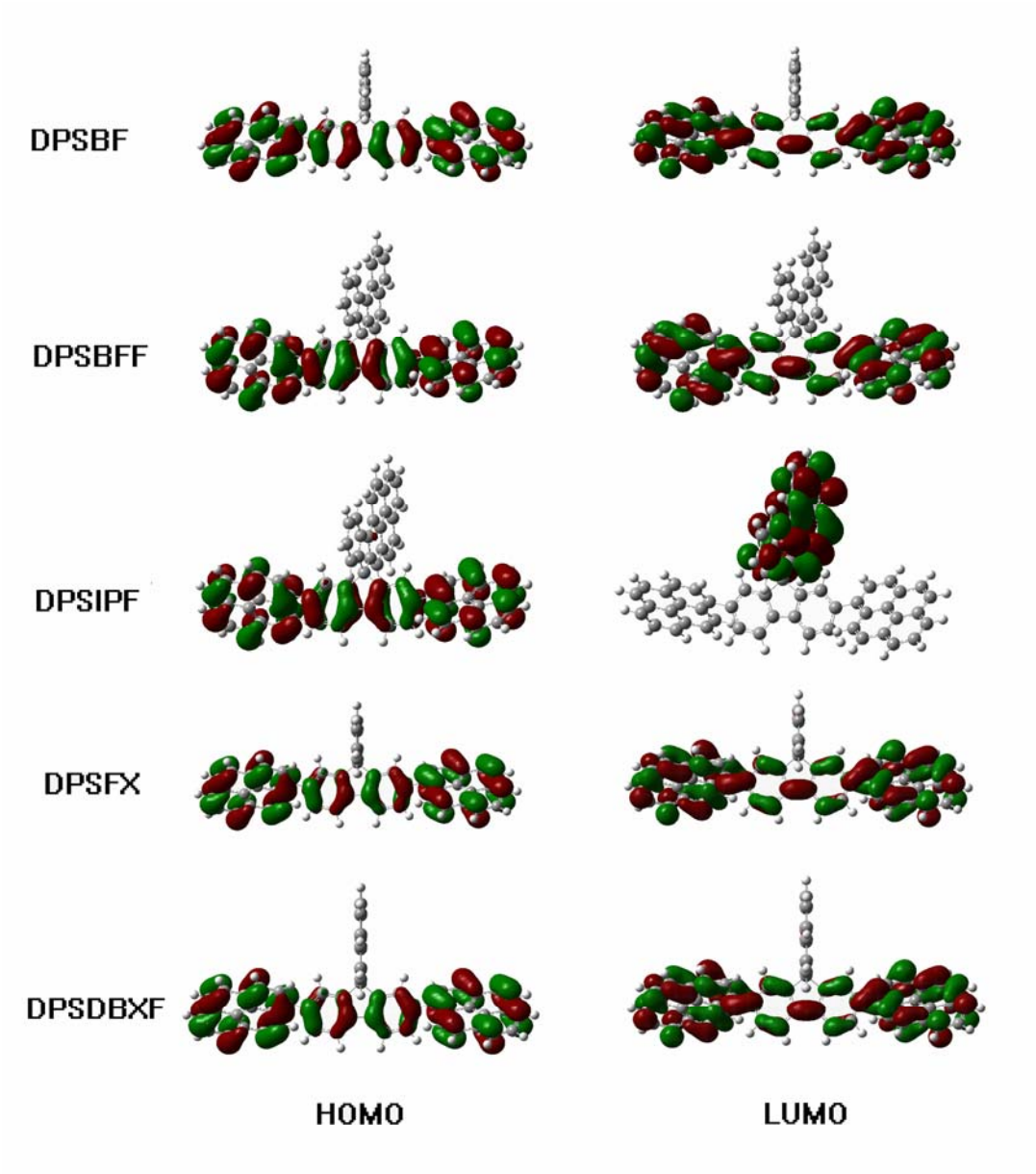

Figure S-3. HOMO-LUMO of materials

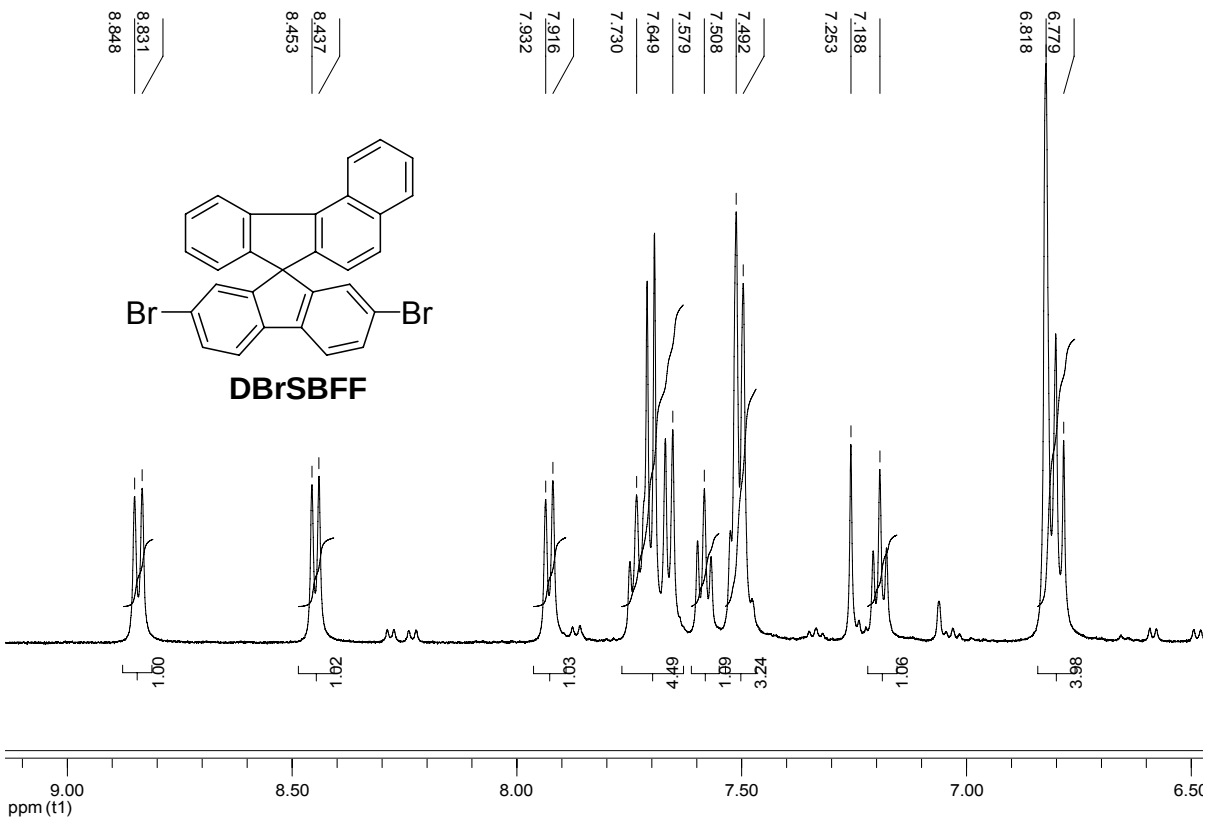

Figure S-4. ^{1}H NMR of DBrSBFF

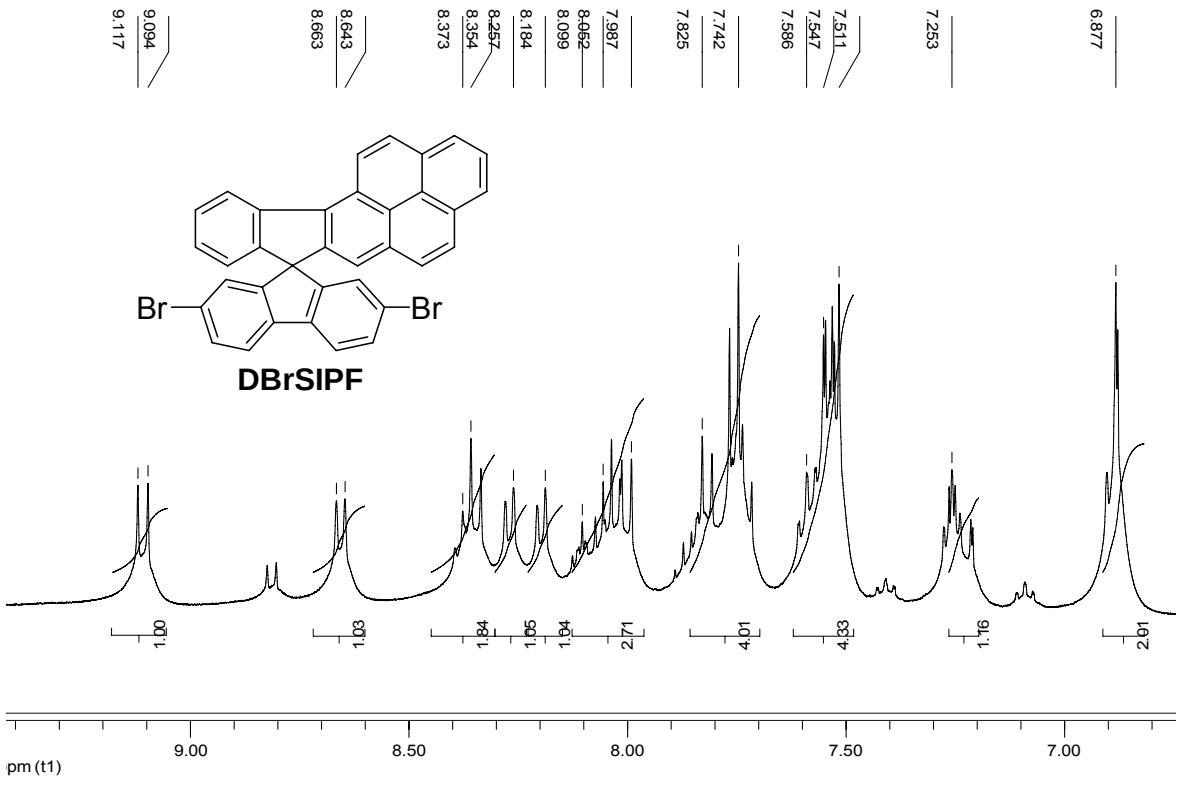

Figure S-5. ^{1}H NMR of DBrSIPF

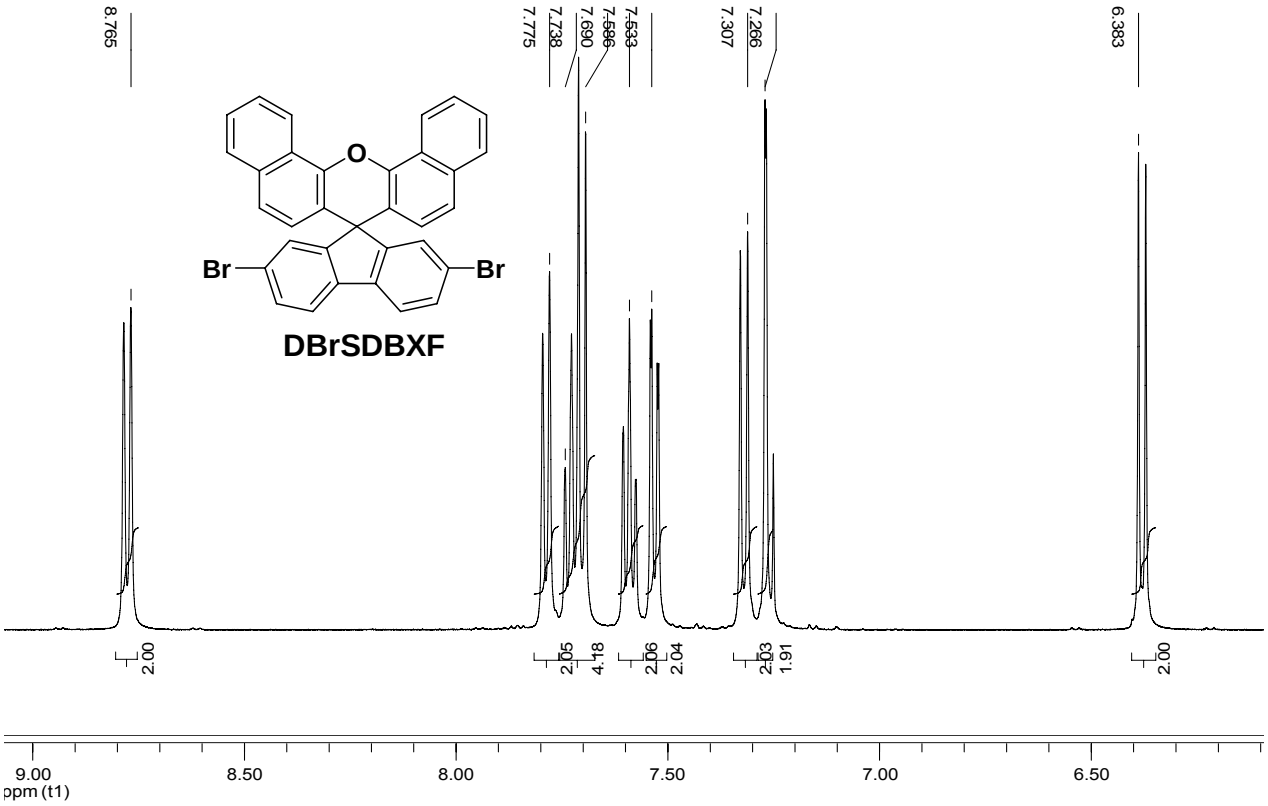

Figure S-6. [1]H NMR of DBrSDBXF

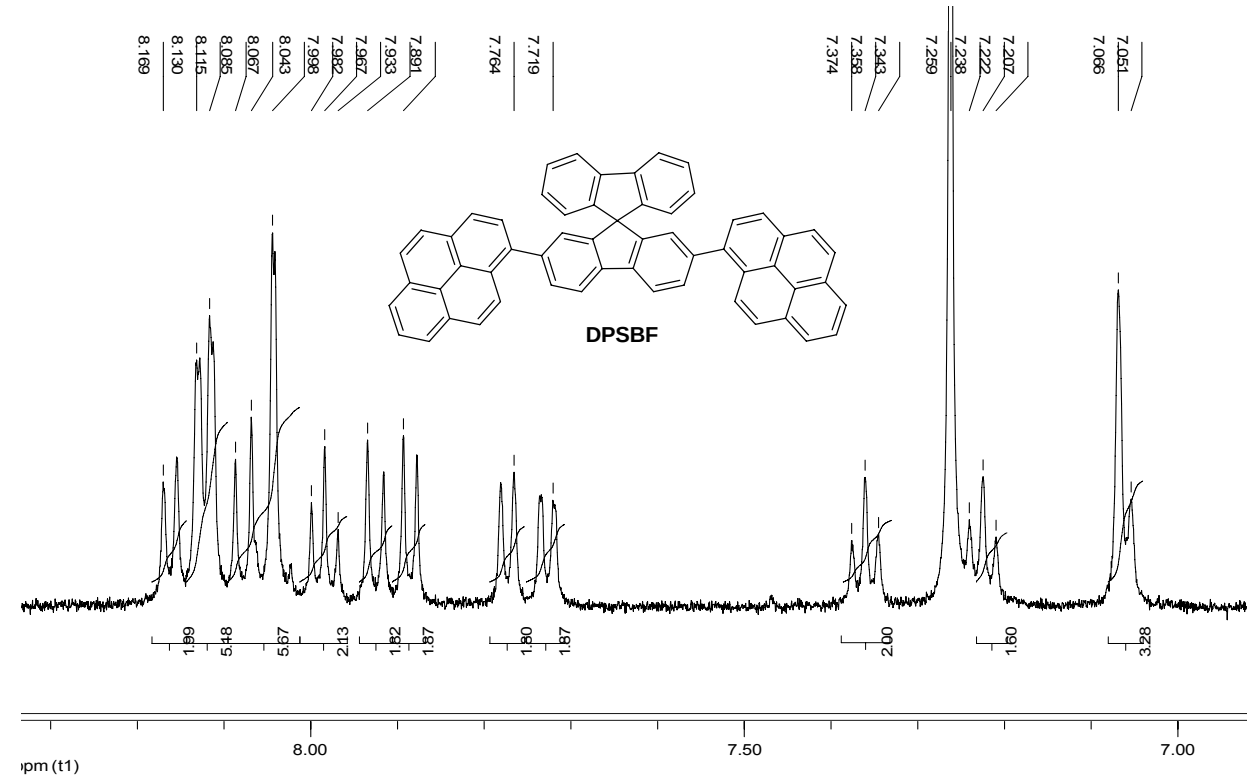

Figure S-7. [1]H NMR of DPSBF

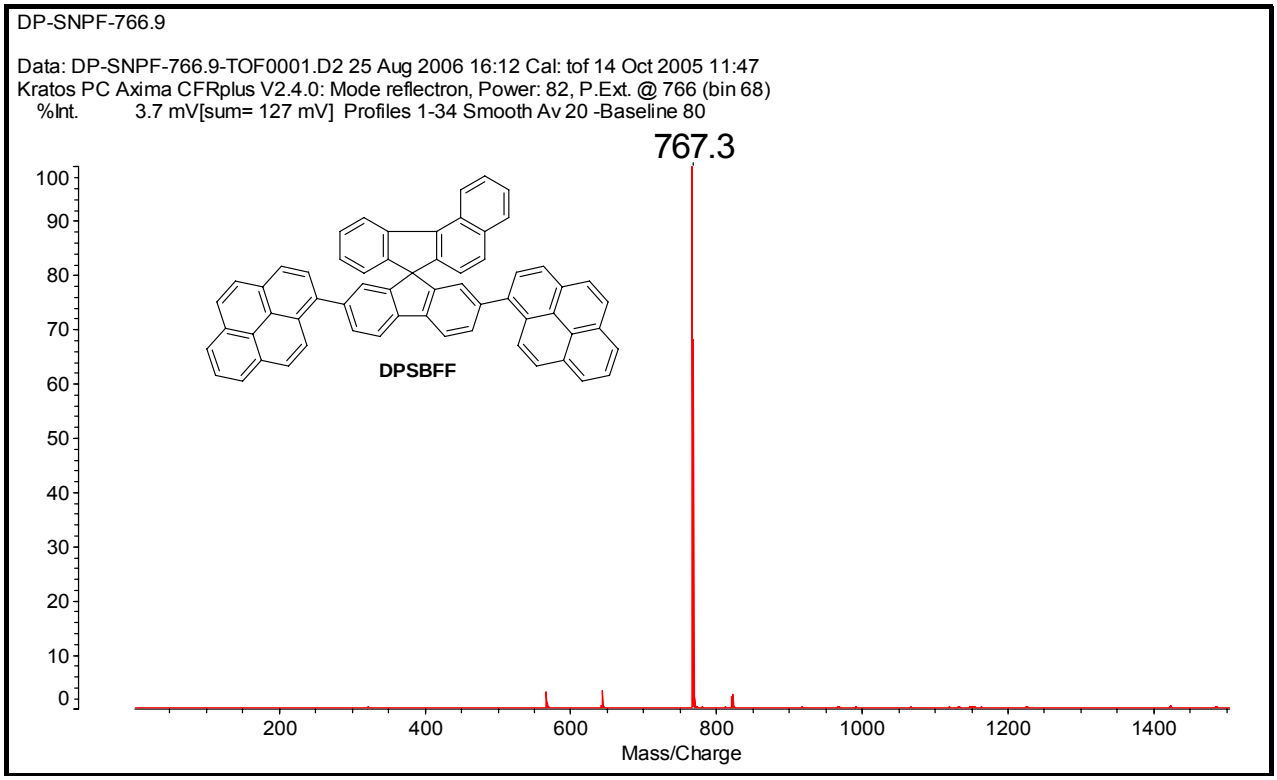

Figure S-8. MALDI-TOF-MS of DPSBFF

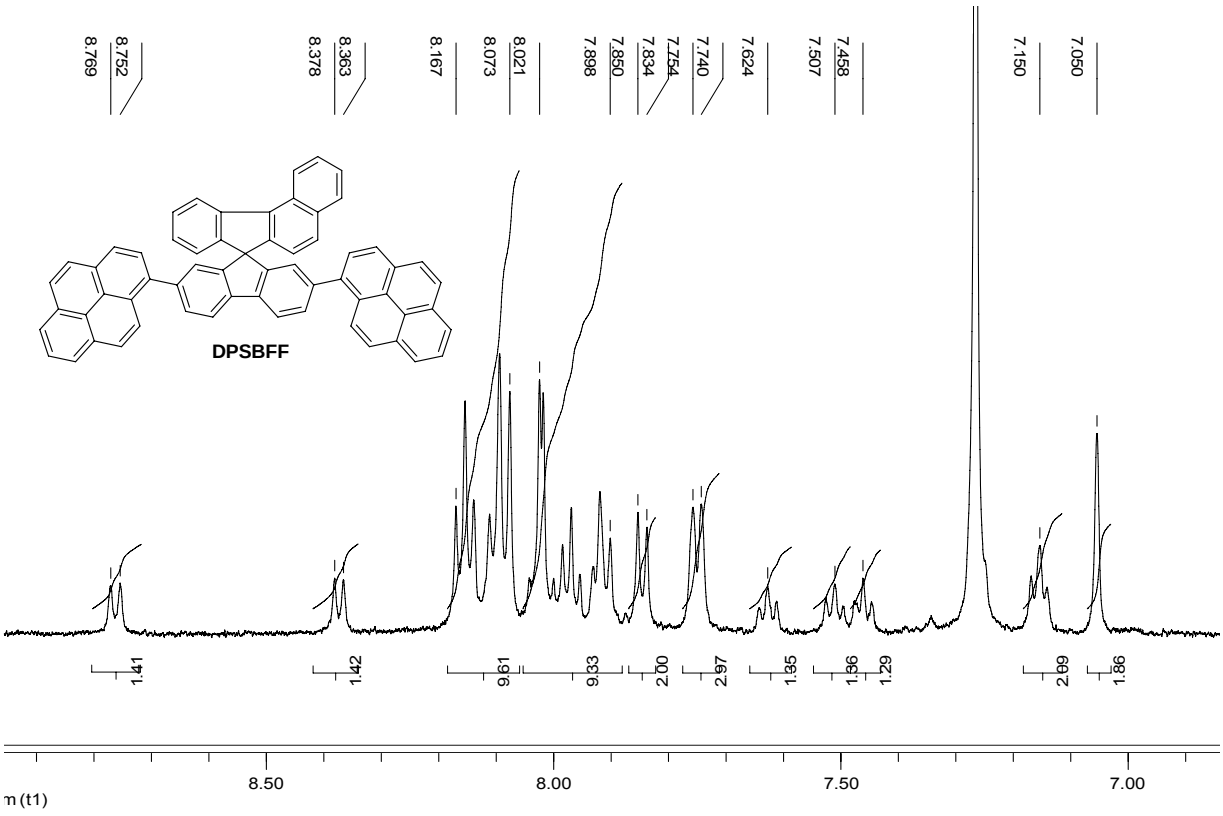

Figure S-9. ^{1}H NMR of DPSBFF

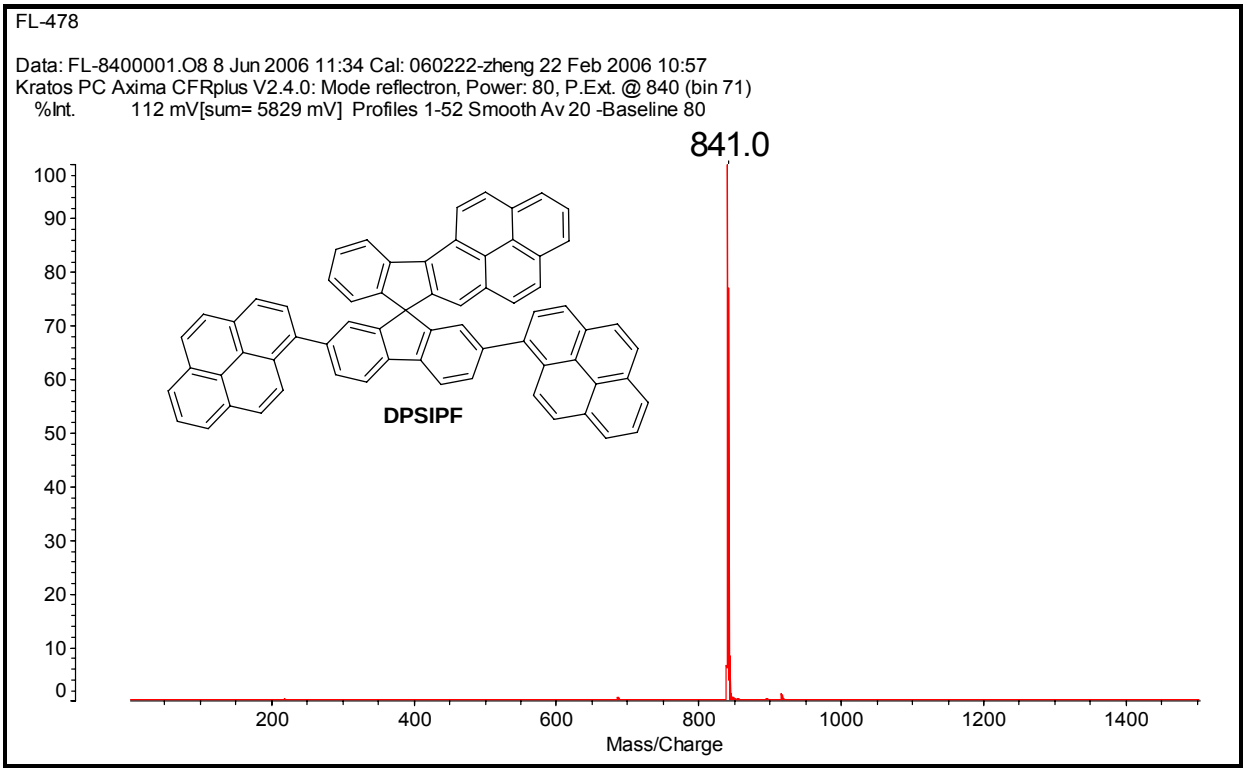

Figure S-10. MALDI-TOF-MS of DPSIPF

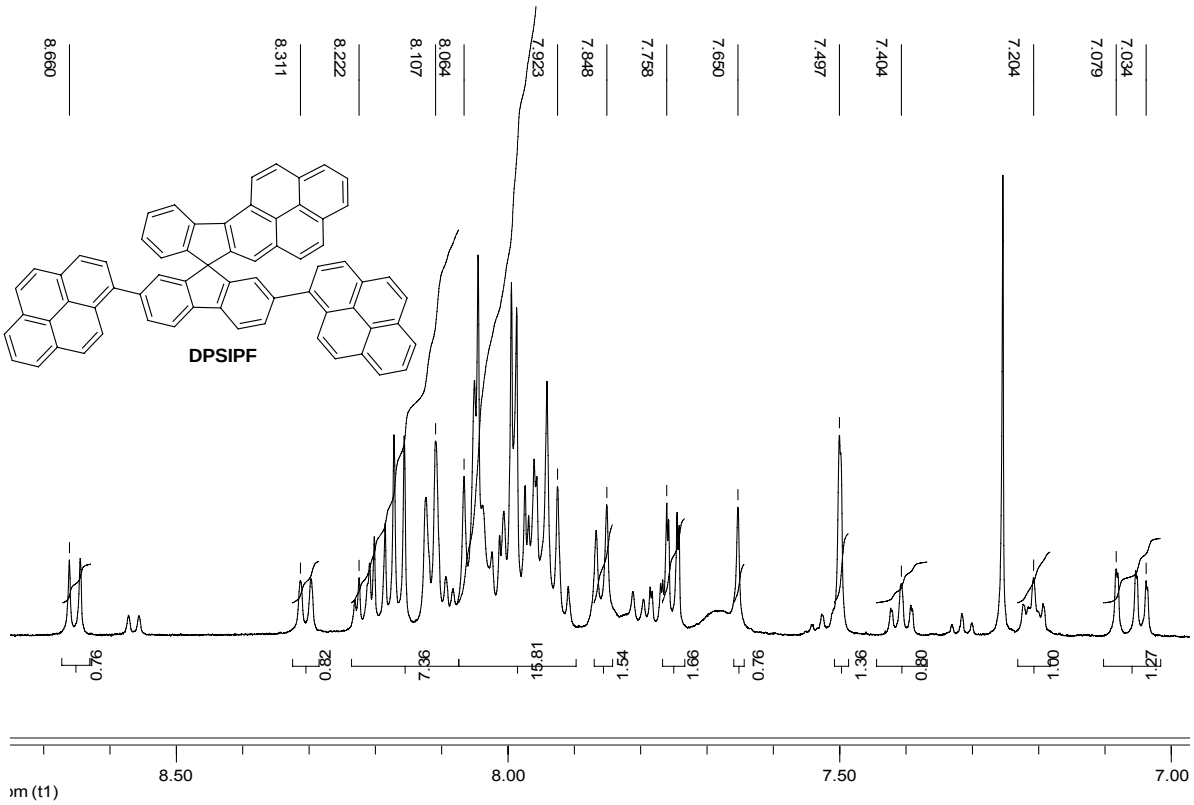

Figure S-11. ^{1}H NMR of DPSIPF

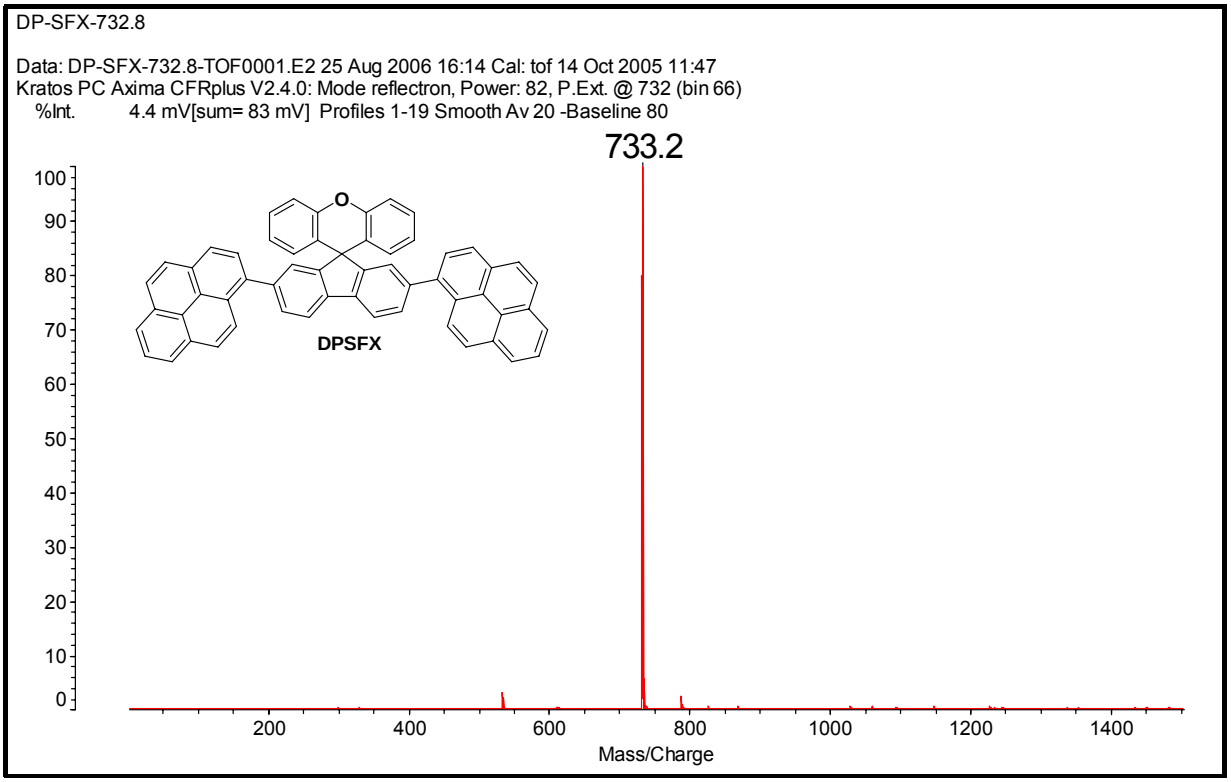

Figure S-12. MALDI-TOF-MS of DPSFX

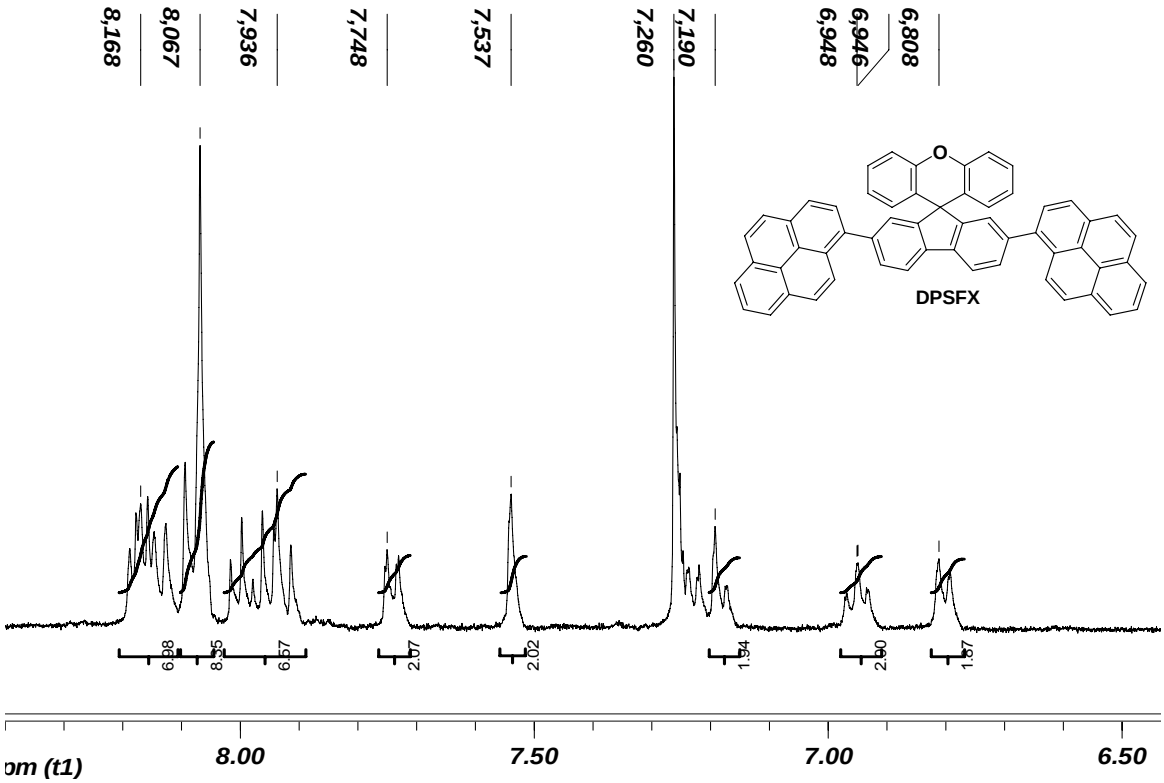

Figure S-13. ^{1}H NMR of DPSFX

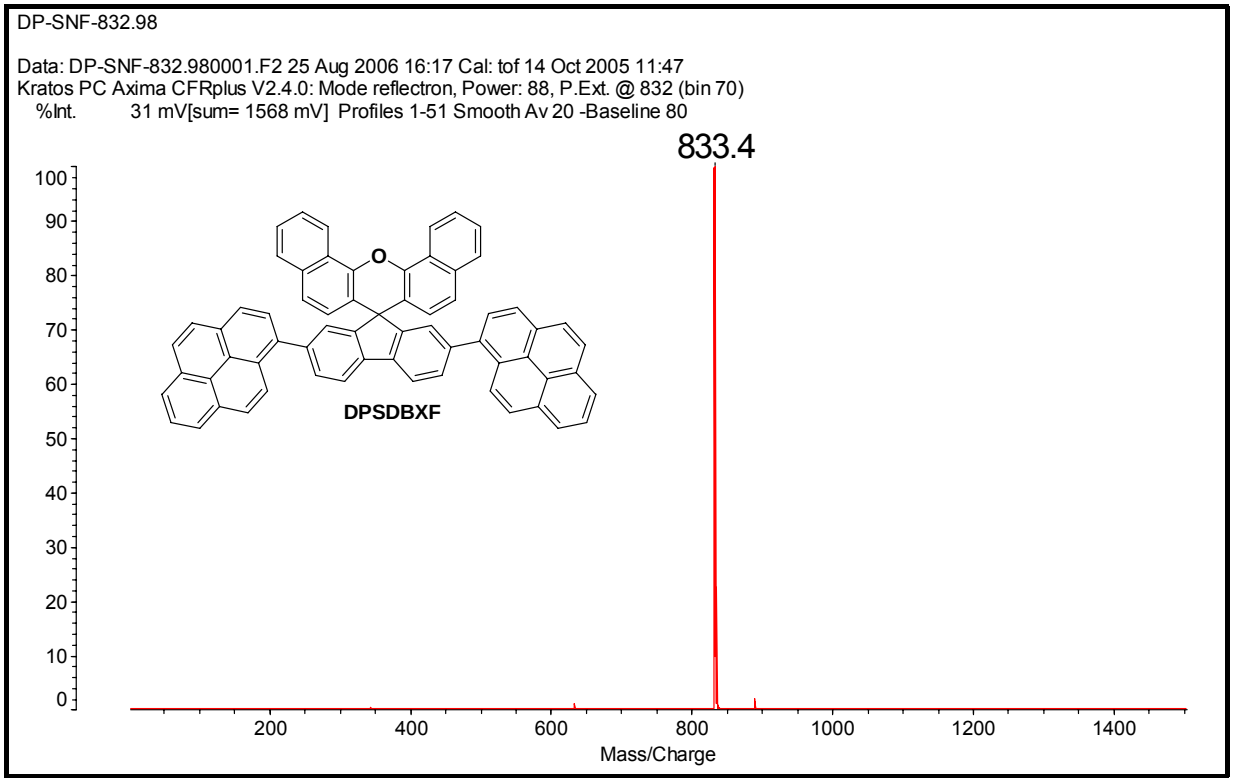

Figure S-14. MALDI-TOF-MS of DPSFDBX

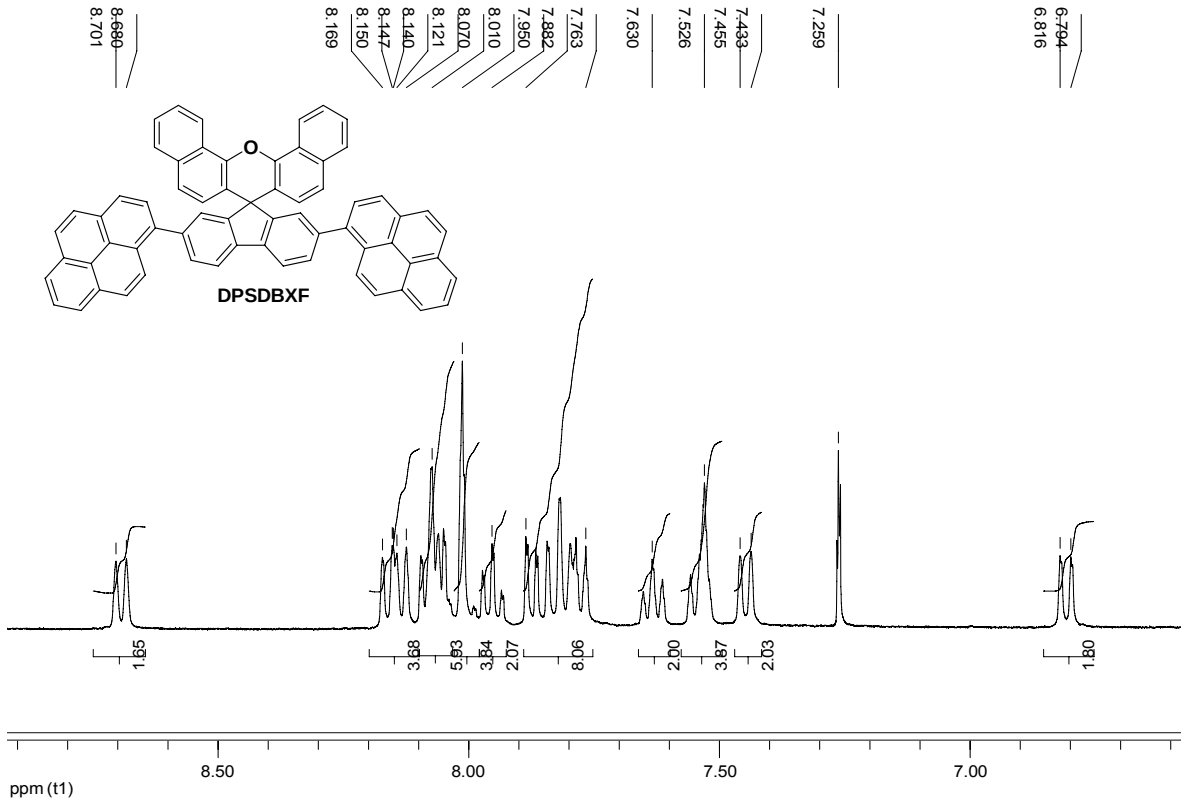

Figure S-15. ^{1}H NMR of DPSDBXF